Petroleum Science 20 (2023) 1843–1856

Contents lists available at ScienceDirect

Petroleum Science

journal homepage: www.keaipublishing.com/en/journals/petroleum-science

Original Paper

Subsection and superposition method for reservoir formation damage evaluation of complex-structure wells

Guan-Cheng Jiang [a, b, e, *], Yi-Zheng Li [a, b], Yin-Bo He [a, b, e], Teng-Fei Dong [a, b], Ke-Ming Sheng [b, c], Zhe Sun [d]

[a] College of Petroleum Engineering, China University of Petroleum (Beijing), Beijing, 102249, China
[b] State Key Laboratory of Petroleum Resources and Prospecting, MOE Key Laboratory of Petroleum Engineering, China University of Petroleum (Beijing), Beijing, 102249, China
[c] College of Artificial Intelligence, China University of Petroleum (Beijing), Beijing, 102249, China
[d] Calgary Centre for Innovative Technology, University of Calgary, Calgary, AB T2N 1N4, Canada
[e] National Engineering Research Center of Oil # Gas Drilling and Completion Technology

A R T I C L E I N F O

Article history:
Received 29 July 2022
Received in revised form
26 November 2022
Accepted 12 January 2023
Available online 13 January 2023

Edited by Jia-Jia Fei

Keywords:
Complex-structure wells
Reservoir formation damage
Reservoir anisotropy
Skin factor
Production prediction model

A B S T R A C T

Kinds of complex-structure wells can effectively improve production, which are widely used. However, in the process of drilling and completion, complex-structure wells with long drilling cycle and large exposed area of reservoir can lead to the fact that reservoir near wellbore is more vulnerable to the working fluid invasion, resulting in more serious formation damage. In order to quantitatively describe the reservoir formation damage in the construction of complex-structure well, taking the inclined well section as the research object, the coordinate transformation method and conformal transformation method are given according to the flow characteristics of reservoir near wellbore in anisotropic reservoir. Then the local skin factor in orthogonal plane of wellbore is deduced. Considering the uneven distribution of local skin factor along the wellbore, the oscillation decreasing model and empirical equation model of damage zone radius distribution along the wellbore direction are established and then the total skin factor model of the whole well is superimposed to realize the reservoir damage evaluation of complex-structure wells. Combining the skin factor model with the production model, the production of complex-structure wells can be predicted more accurately. The two field application cases show that the accuracy of the model can be more than 90%, which can also fully reflect the invasion characteristics of drilling and completion fluid in any well section of complex-structure wells in anisotropic reservoir, so as to further provide guidance for the scientific establishment of reservoir production system.

1. Introduction

With the large-scale exploitation of oil and gas, most of the remaining conventional resources are located in the reservoirs with extremely complex geological conditions and poor physical properties, whose permeability and porosity are mainly low or ultra-low (Kantaatmadja et al., 2019; Alghazal et al., 2020; He et al., 2022). Developing by vertical wells in such reservoirs always has a lower production per well, making effective development difficult (Smith et al., 1981; Poe Jr et al., 2012; Wu et al., 2020). Complex-structure wells are series of wells with the basic characteristics of horizontal wells, including horizontal well, dual horizontal well, extended-reach well, multilateral well, herringbone well, connected well and so on (Joshi, 1987; Aadnoy et al., 2009; Mehrabi et al., 2014). Compared with vertical wells and cluster wells, complex-structure wells effectually increase the exposed area of oil and gas and the controlled reserves of wells, thus greatly improving the production and production efficiency (Joshi, 1994; Ahmadi et al., 2020; Hu et al., 2022). For example, the drainage area of oil and gas controlled by a horizontal well with a horizontal section of 100 m is three times that of a vertical well, and this increase in production is more prominent in fractured reservoirs (Joshi, 2003; Dulkarnaev

* Corresponding author. College of Petroleum Engineering, China University of Petroleum (Beijing), Beijing, 102249, China.
E-mail address: jgc5786@126.com (G.-C. Jiang).

https://doi.org/10.1016/j.petsci.2023.01.010

et al., 2021). Moreover, it can effectively reduce the area of well pads and capital construction costs, so complex-structure wells are more widely used in offshore oilfield exploitation (Hasan et al., 2009; Jenny and Lunati, 2009; Hassan et al., 2020).

Although the use of complex-structure wells increase the oil drainage area and have significant benefits in production, the area of working fluid contacting the reservoir is larger and the contact time is longer due to the complex-structure wells' trajectory (Moreno et al., 2006; Sau et al., 2014; Klemetsdal et al., 2017), or multiple branch wells and the long well construction cycle, which leads to greater damage to the reservoir (Joshi, 1994, 2003; Jiang et al., 2021). Therefore, it is necessary to study and quantitatively evaluate the reservoir formation damage of complex-structure wells caused during the well construction.

At present, many scholars have studied the skin factor model (Thomas et al., 1998; Basquet et al., 1998) as well as the impact of reservoir damage on production of highly inclined directional wells, horizontal wells and other complex-structure wells (Joshi, 1986). Most models, based on the optimization of Hawkins skin factor equation, regard the damage zone radius along the direction from the toe to the root of the wellbore as a constant distribution, linear distribution and parabolic distribution respectively (Zhang and Yan, 2001; An et al., 2008; Sun, 2020). Some scholars (An et al., 2008; Wu et al., 2008; Wang et al., 2009) regard the skin factor (damage zone) as a constant along the direction of wellbore. Zhang and Yan (2001) improved the Hawkins skin factor model for highly inclined wells (Hawkins, 1956) with reference to Frick Economides (Frick and Economides, 1993) model, in which the skin factor is regarded as linear decrease along the wellbore, but the anisotropy of reservoir is not considered. Sun (2020) optimized the skin factor model of Furui Zhu Hill (Furui et al., 2003, 2004) by assuming that the damage zone distribution along the wellbore of horizontal well is a parabolic decreasing type, but did not give the calculation method of the maximum damage zone radius assumed in the skin factor model, which is difficult to be obtained directly from field. Additionally, due to many factors such as reservoir physical properties, drilling and completion fluid performance, construction parameters and so on, the damage zone shape near the well of complex-structure wells cannot be a uniform cylinder or circular truncated cone from a three-dimensional perspective, in another words, the distribution of skin factor along the wellbore direction is not a simple constant, linear or parabolic distribution described in the above model.

In this paper, a skin factor model for evaluating the reservoir damage of complex-structure wells during drilling and completion in the anisotropic reservoir is established by analytic technique based on subsection and superposition method, which gives a way for converting anisotropic reservoir to isotropic reservoir, uneven distribution model of reservoir damage zone radius along the wellbore, local and total skin factor model, equivalent damaged permeability and damage zone radius of complex-structure wells. The model can be used to evaluate the reservoirs damage of complex-structure wells caused by the working fluid invasion during the well construction. Considering the skin factor model in the oil and gas production prediction, it can provide more accurate guidance for the production prediction of complex-structure wells. The two field cases application indicate that the production prediction model after considering reservoir formation damage has higher accuracy to more than 90%.

2. Methodology

Due to overbalance drilling or completion, reservoir near the wellbore of complex-structure well is invaded by working fluid, causing reservoir formation damage. Before modeling, the following assumptions are proposed in order to make the model more reasonable.

a. The temperature, fluid density and viscosity of the reservoir are considered to be constant.
b. The compressibility of working fluid and reservoir fluid is not considered.
c. The influence of gravity on the invasion of working fluid into the reservoir is not considered.
d. The filtration of drilling fluid at the bit is not considered. There are only static filtration and dynamic filtration of drilling fluid during drilling.
e. There are no large or special fractures in the reservoir around the well section calculated.

2.1. Transforming anisotropic reservoir into equivalent isotropic reservoir

As the uneven distribution of *in-situ* stress, there is generally anisotropy in the reservoir and the direction of the maximum permeability is generally consistent with the direction of the maximum horizontal principal stress (Liu et al., 2005). In order to quantitatively evaluate the reservoir damage of complex-structure wells, the inclined section is taken as the research object, so the vertical section and horizontal section are two special cases. Assuming that there is an inclined well section with a length of L_i and a wellbore radius of r_w in an anisotropic reservoir with a reservoir thickness of h and the *oxyz* coordinate system is defined, as shown in Fig. 1a, where *oz* is perpendicular to the formation plane and *oxy* plane is horizontal. The permeability in the *xyz* direction of the three coordinate axes are the maximum horizontal permeability K_x, the minimum horizontal permeability K_y and the formation vertical permeability K_z ($K_x > K_y > K_z$). The well inclination angle of this inclined well section is θ and the azimuth angle is φ, where $0 = \theta \leq \pi$ and $0 = \varphi \leq 2\pi$.

In the *oxyz* coordinate system, the three-dimensional steady-state fluid flow partial differential equation of single-phase incompressible liquid in the reservoir is:

$$K_x\frac{\partial^2 P}{\partial x^2}+K_y\frac{\partial^2 P}{\partial y^2}+K_z\frac{\partial^2 P}{\partial z^2}=0 \tag{1}$$

where K_x, K_y and K_z are respectively formation permeability in three coordinate axes of x, y and z, m^2; and P is formation pressure, Pa.

Let $x=\sqrt[6]{\frac{K_x^2}{K_yK_z}}x'$, $y=\sqrt[6]{\frac{K_y^2}{K_xK_z}}y'$ and $z=\sqrt[6]{\frac{K_z^2}{K_xK_y}}z'$ be substituted into Eq. (1) to obtain:

$$\frac{\partial^2 P}{\partial x'^2}+\frac{\partial^2 P}{\partial y'^2}+\frac{\partial^2 P}{\partial z'^2}=0 \tag{2}$$

Eq. (2) represents the three-dimensional steady-state fluid flow partial differential equation in the $ox'y'z'$ coordinate system. Using the above relationship to make coordinate transformation, the *oxyz* coordinate system is transformed into the $ox'y'z'$ coordinate system, that is:

$$\begin{bmatrix} x' \\ y' \\ z' \end{bmatrix}=\begin{bmatrix} a & 0 & 0 \\ 0 & b & 0 \\ 0 & 0 & c \end{bmatrix}\begin{bmatrix} x \\ y \\ z \end{bmatrix} \tag{3}$$

where $a=\frac{\sqrt{K_yK_z}}{\sqrt[3]{K_xK_yK_z}}$, $b=\frac{\sqrt{K_xK_y}}{\sqrt[3]{K_xK_yK_z}}$ and $c=\frac{\sqrt{K_xK_z}}{\sqrt[3]{K_xK_yK_z}}$.

Then in the $ox'y'z'$ coordinate system, the permeability tensor is

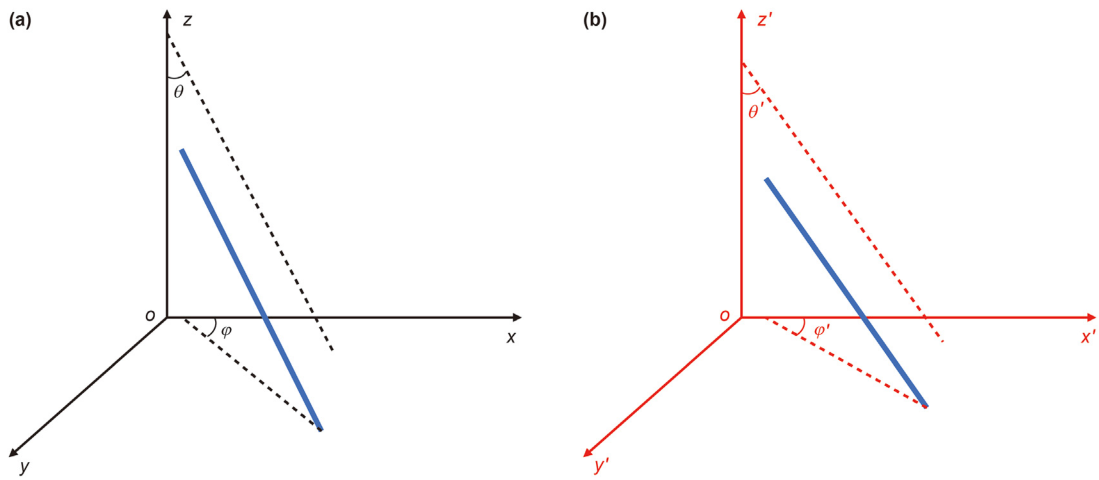

Fig. 1. An inclined well section in: (**a**) anisotropic reservoir under *oxyz* coordinate system; (**b**) equivalentisotropic reservoir under $ox'y'z'$ coordinate system.

transformed into:

$$\mathbf{K}' = \begin{bmatrix} \sqrt[3]{K_x K_y K_z} & 0 & 0 \\ 0 & \sqrt[3]{K_x K_y K_z} & 0 \\ 0 & 0 & \sqrt[3]{K_x K_y K_z} \end{bmatrix} \tag{4}$$

It can be seen that after coordinate transformation, the original anisotropic permeability space is transformed into an equivalent isotropic permeability space, as shown in Fig. 1b.

In the isotropic coordinate space, the new deviation angle θ', azimuth angle φ', wellbore length L_i', wellbore radius r_w' and permeability K' can be expressed as:

$$\begin{aligned} \theta' &= \arctan\left(\tan\theta \frac{\sqrt{a^2\cos^2\varphi + b^2\sin^2\varphi}}{c}\right) \\ \varphi' &= \arctan\left(\frac{b}{a}\tan\varphi\right) \\ L_i' &= L_i\sqrt{c^2\cos^2\theta + \left(a^2\cos^2\varphi + b^2\sin^2\varphi\right)\sin^2\theta} \\ r_w' &= r_w\sqrt{c^2\cos^2\theta + \left(a^2\cos^2\varphi + b^2\sin^2\varphi\right)\sin^2\theta} \\ K' &= \sqrt[3]{K_x K_y K_z} = K\bullet\beta^{\frac{1}{3}} \end{aligned} \tag{5}$$

where β is anisotropic coefficient of formation, $\beta = \sqrt{\frac{K_h}{K_z}}$; and K_h is horizontal permeability of formation, $K_h = \sqrt{K_x K_y}$, m^2.

The isobars around the wellbore are always distributed in the plane perpendicular to the wellbore and the reservoir damage is directly related to the formation pressure. Here, rotate the $ox'y'z'$ coordinate system to make one of the coordinate axes parallel to the axial direction of the inclined wellbore section, so that the pressure distribution of the formation around the wellbore can be expressed by quantities in two directions in the same coordinate plane. For the coordinates in Fig. 1b, in order to make the coordinate axis z' parallel to the wellbore direction, take the z' axis direction as the axis and rotate the $ox'z'$ plane ($oy'z'$ plane) clockwise φ' angle to get a new $ox''y''z''$ coordinate system, and then take the y'' axis direction as the axis and rotate the $ox''y''$ plane ($oy''z''$ plane) clockwise θ' angle to get a new $ox'''y'''z'''$ coordinate system, as shown in Fig. 2 and Fig. 3. The conversion relationship from *oxyz* coordinate system to $ox'''y'''z'''$ coordinate system is (Besson, 1990):

$$\begin{bmatrix} x''' \\ y''' \\ z''' \end{bmatrix} = \begin{bmatrix} \cos\theta'\cos\varphi' & \cos\theta'\sin\varphi' & \sin\theta' \\ -\sin\varphi' & \cos\varphi' & 0 \\ -\sin\theta'\cos\varphi' & -\sin\theta'\sin\varphi' & \cos\theta' \end{bmatrix} \begin{bmatrix} ax \\ by \\ cz \end{bmatrix} \tag{6}$$

Using $ou'v'w'$ to represent the transformed coordinate axis $x'''y'''z'''$, then the reservoir is isotropic in the $ou'v'w'$ coordinate system, where the w' axis is always parallel to the inclined well section studied and the $ou'v'$ plane is perpendicular to the wellbore, then the distribution of formation pressure field or damage near the inclined well section can be represented in an $ou'v'$ plane. Accordingly, the *ouvw* coordinate system is the coordinate system obtained by rotating the *oxyz* coordinate system. The *w* axis is always parallel to the inclined well section studied and any *ouv* plane is perpendicular to the wellbore. The reservoir represented below is an anisotropic reservoir with unconverted permeability. In the *ouv* plane, it can also represent the flow characteristics of the stratum near the inclined well section or the distribution of wellbore damage. The conversion relationship between the two coordinate systems and the permeability conversion relationship are shown in Eqs. (7)–(10) respectively.

$$\begin{bmatrix} u' \\ v' \\ w' \end{bmatrix} = \begin{bmatrix} \cos\theta'\cos\varphi' & \cos\theta'\sin\varphi' & \sin\theta' \\ -\sin\varphi' & \cos\varphi' & 0 \\ -\sin\theta'\cos\varphi' & -\sin\theta'\sin\varphi' & \cos\theta' \end{bmatrix} \begin{bmatrix} ax \\ by \\ cz \end{bmatrix} \tag{7}$$

$$\begin{bmatrix} K_{u'} \\ K_{v'} \\ K_{w'} \end{bmatrix} = \begin{bmatrix} \cos^2\theta'\cos^2\varphi' & \cos^2\theta'\sin^2\varphi' & \sin^2\theta' \\ \sin^2\varphi' & \cos^2\varphi' & 0 \\ \sin^2\theta'\cos^2\varphi' & \sin^2\theta'\sin^2\varphi' & \cos^2\theta' \end{bmatrix} \begin{bmatrix} a^2 K_x \\ b^2 K_y \\ c^2 K_z \end{bmatrix} \tag{8}$$

$$\begin{bmatrix} u \\ v \\ w \end{bmatrix} = \begin{bmatrix} \cos\theta\cos\varphi & \cos\theta\sin\varphi & \sin\theta \\ -\sin\varphi & \cos\varphi & 0 \\ -\sin\theta\cos\varphi & -\sin\theta\sin\varphi & \cos\theta \end{bmatrix} \begin{bmatrix} x \\ y \\ z \end{bmatrix} \tag{9}$$

$$\begin{bmatrix} K_u \\ K_v \\ K_w \end{bmatrix} = \begin{bmatrix} \cos^2\theta\cos^2\varphi & \cos^2\theta\sin^2\varphi & \sin^2\theta \\ \sin^2\varphi & \cos^2\varphi & 0 \\ \sin^2\theta\cos^2\varphi & \sin^2\theta\sin^2\varphi & \cos^2\theta \end{bmatrix} \begin{bmatrix} K_x \\ K_y \\ K_z \end{bmatrix} \tag{10}$$

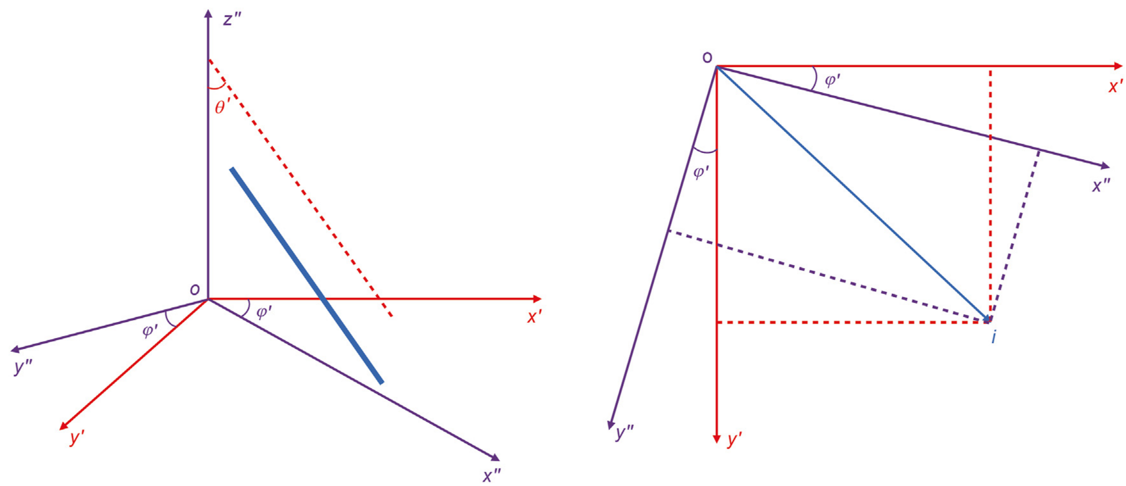

Fig. 2. Conversion of this inclined well section in isotropic reservoir under $ox''y''z''$ coordinate system.

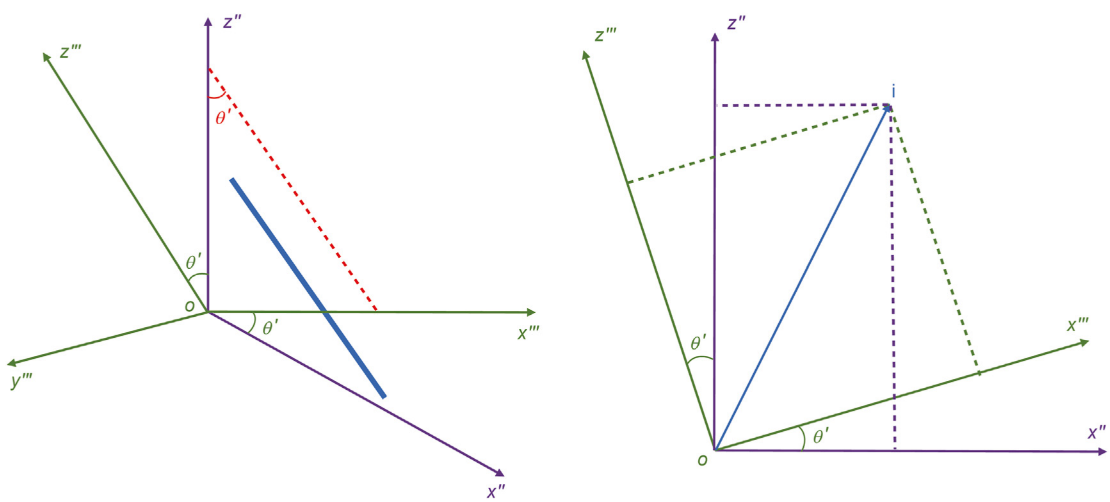

Fig. 3. Conversion of this inclined well section in isotropic reservoir under $ox'''y'''z'''$ coordinate system.

2.2. Damage zone distribution near single well section of complex-structure wells

In the *ouv* plane under the *ouvw* coordinate system of anisotropic reservoir, w is a constant, so the steady-state flow equation of reservoir near the inclined well section can be expressed as:

$$K_u\frac{\partial^2 P}{\partial u^2}+K_v\frac{\partial^2 P}{\partial v^2}=0 \tag{11}$$

Eq. (11) is a common second-order linear elliptic partial differential equation, whose internal boundary condition is:

$$\begin{cases} u^2+v^2=r_{\mathrm{w}}^2 \\ P=P_{\mathrm{wf}} \end{cases} \tag{12}$$

where P_{wf} is bottom hole pressure, Pa.

Through Eqs. (11) and (12), it can be found that in anisotropic reservoirs, the isobars around the wellbore are a series of concentric ellipses (Peaceman, 1983). The closer the ellipse is to the wellbore, the closer the ratio of its major axis to its minor axis is to 1, until it reaches the circular wellbore. Fig. 4 shows the distribution and damage of wellbore isobars in anisotropic reservoir.

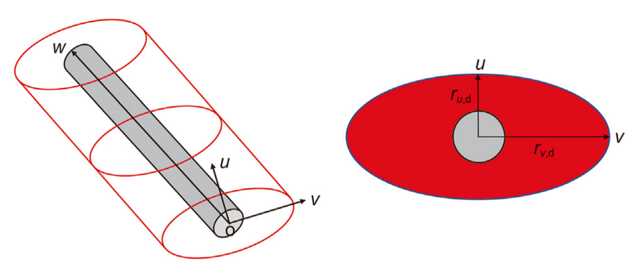

Fig. 4. Schematic diagram of isobaric line and reservoir damage near wellbore in anisotropic reservoir.

After coordinate transformation, the anisotropic reservoir is transformed into an equivalent isotropic reservoir under the new coordinate system $ou'v'w'$. In the orthogonal plane of the wellbore, the transformation relationship between the two coordinate systems is:

$$\begin{bmatrix} u' \\ v' \end{bmatrix} = \begin{bmatrix} \sqrt[4]{\frac{K_v}{K_u}} & 0 \\ 0 & \sqrt[4]{\frac{K_u}{K_v}} \end{bmatrix} \begin{bmatrix} u \\ v \end{bmatrix} \tag{13}$$

Then the steady-state fluid flow equation in the orthogonal plane $ou'v'$ of the wellbore changes from Eq. (11) to:

$$\frac{\partial^2 P}{\partial u'^2} + \frac{\partial^2 P}{\partial v'^2} = 0 \tag{14}$$

Eq. (14) is a Laplace equation, and the corresponding inner boundary condition is changed from Eq. (12) to:

$$\begin{cases} \dfrac{u'^2}{\left[r_w\left(\dfrac{K_v}{K_u}\right)^{\frac{1}{4}}\right]^2} + \dfrac{v'^2}{\left[r_w\left(\dfrac{K_u}{K_v}\right)^{\frac{1}{4}}\right]^2} = 1 \\ P = P_{wf} \end{cases} \tag{15}$$

Through Eq. (14) and boundary condition Eq. (15), it can be found that in the equivalent isotropic reservoir, isobars around the wellbore are a series of confocal concentric ellipses and the wellbore shape is converted into an ellipse with the focus on the v' axis. The farther away from the wellbore, the closer the ratio of the major axis to the minor axis of the elliptical isobars is to 1 and the closer the shape is to a circle. The isobaric distribution and damage in the orthogonal plane of the wellbore are shown in Fig. 5.

2.3. Local skin factor of complex-structure wells

Conformal transformation (Kang et al., 2021) is introduced to solve the Laplace equation of elliptic internal boundary conditions shown in Eqs. (14) and (15), and the transformation function is taken:

$$A = l \cdot \mathrm{ch}B \tag{16}$$

where $A = x + iy$ and $B = \zeta + i\eta$.

Convert plane A in $ou'v'$ coordinate system to plane B in $o\zeta\eta$ coordinate system, so that the elliptic potential line in plane A is transformed into the linear potential line in plane B, as shown in Fig. 6. The coordinate transformation relationship is as follows:

$$\begin{cases} u' = l \cdot \mathrm{ch}\zeta \cdot \sin\eta \\ v' = l \cdot \mathrm{sh}\zeta \cdot \cos\eta \end{cases} \tag{17}$$

where shζ is hyperbolic sine function, $\mathrm{sh}\zeta = \frac{1}{2}(e^{\zeta} + e^{-\zeta})$. ch$\zeta$ is hyperbolic cosine function, $\mathrm{ch}\zeta = \frac{1}{2}(e^{\zeta} - e^{-\zeta})$.

According to Eq. (17), the short axis and long axis of the

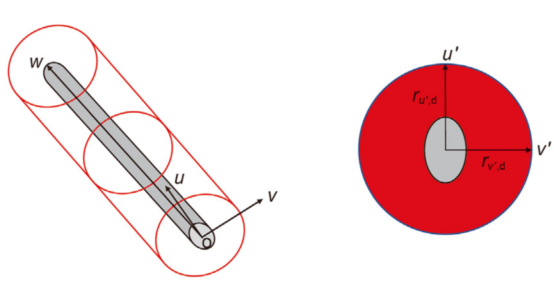

Fig. 5. Schematic diagram of isobaric line and reservoir damage near wellbore in anisotropic reservoir.

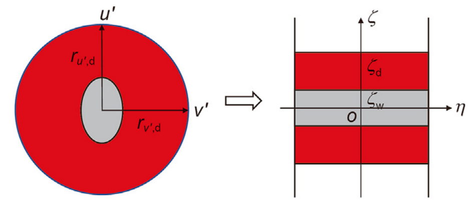

Fig. 6. Conformal transformation in the orthogonal plane of wellbore in isotropic reservoir.

corresponding elliptic isobar in Fig. 6 are: $l \cdot \mathrm{ch}\zeta$ and $l \cdot \mathrm{sh}\zeta$. Combined Eq. (15), the minor axis and major axis of the elliptical wellbore boundary are respectively:

$$\begin{cases} l \cdot \mathrm{ch}\zeta_w = r_w\left(\dfrac{K_v}{K_u}\right)^{\frac{1}{4}} \\ l \cdot \mathrm{sh}\zeta_w = r_w\left(\dfrac{K_u}{K_v}\right)^{\frac{1}{4}} \end{cases} \tag{18}$$

From Eq. (18), $l = r_w\sqrt{\sqrt{\frac{K_v}{K_u}} - \sqrt{\frac{K_u}{K_v}}}$ and $\zeta_w = \ln\sqrt{\frac{1+\sqrt{\frac{K_u}{K_v}}}{1-\sqrt{\frac{K_u}{K_v}}}}$ can be gotten.

Take the average value of the long axis and short axis of the elliptic isobar as the average radius of the elliptical wellbore:

$$\overline{r} = \frac{l \cdot \mathrm{ch}\zeta + l \cdot \mathrm{sh}\zeta}{2} = \frac{l}{2}e^{\zeta} \tag{19}$$

According to simultaneous Eqs. (18) and (19), the average radius of elliptic wellbore in equivalent isotropic reservoir is:

$$\overline{r'_w} = \frac{l}{2}e^{\zeta_w} = \frac{r_w}{2}\left(1 + \sqrt{\frac{K_u}{K_v}}\right)\sqrt[4]{\frac{K_v}{K_u}} \tag{20}$$

In anisotropic reservoir, in order to solve the boundary of elliptic damage zone, the long axis of ellipse is defined as damage zone radius. Convert it to equivalent isotropic reservoir according to Eq. (13), which is:

$$r'_{v,d} = \sqrt[4]{\frac{K_u}{K_v}}\, r_{v,d} = l \cdot \mathrm{ch}\zeta_d \tag{21}$$

where $r_{v,d}$ is the damage zone radius in anisotropic reservoir, m; and $r'_{v,d}$ is the damage zone radius in equivalent isotropic reservoir.

From the above equation, ζ_d is:

$$\zeta_d = \ln\left(\frac{\sqrt{\frac{K_u}{K_v}} \cdot r_{v,d}}{r_w\sqrt{1 - \frac{K_u}{K_v}}} + \sqrt{\frac{\frac{K_u}{K_v} \cdot r_{v,d}^2}{r_w^2\left(1 - \frac{K_u}{K_v}\right)} - 1}\right) \tag{22}$$

Substituting Eq. (21) into Eq. (19), the average radius of the elliptical damage zone boundary in the equivalent isotropic reservoir is:

$$\overline{r'_d} = \frac{\sqrt[4]{\frac{K_u}{K_v}} \cdot r_{v,d}}{2} + \frac{r_w}{2}\sqrt{\sqrt{\frac{K_u}{K_v}}\frac{r_{v,d}^2}{r_w^2} - \sqrt{\frac{K_v}{K_u}} + \sqrt{\frac{K_u}{K_v}}} \tag{23}$$

Replace the average wellbore radius Eq. (20) and the average damage zone radius Eq. (23) into Hawkins skin factor equation, then the skin factor of the damaged zone in the orthogonal plane of a wellbore near the inclined wellbore section is obtained, as shown in Eqs. (24) and (25).

$$S_{\mathrm{d}}=\frac{\beta h'}{L'}\left(\frac{K'}{K'_{\mathrm{d}}}-1\right)\ln\frac{r'_{\mathrm{d}}}{r'_{\mathrm{w}}} \tag{24}$$

$$S_{\mathrm{di}}(w)=\frac{\beta h'}{L'_{\mathrm{i}}}\left(\frac{K'}{K'_{\mathrm{d}}}-1\right)\ln\left(\frac{\sqrt{\frac{K_u}{K_v}}\cdot\frac{r_{\mathrm{d}}(w)}{r_{\mathrm{w}}}+\sqrt{\frac{K_u}{K_v}\frac{r_{\mathrm{d}}^2(w)}{r_{\mathrm{w}}^2}+\frac{K_u}{K_v}-1}}{1+\sqrt{\frac{K_u}{K_v}}}\right) \tag{25}$$

where $K^{'}$ is the equivalent permeability in equivalent isotropic reservoir, m^2; $K^{'}_{\mathrm{d}}$ is the equivalent permeability of damage zone in equivalent isotropic reservoir, m^2; $r^{'}_{\mathrm{d}}$ is the equivalent radius of damage zone in equivalent isotropic reservoir, m; S_{d} is skin factor; and $S_{\mathrm{d}}(w)$ is the local skin factor in the orthogonal plane w of wellbore.

Integrating Eq. (25) on the length of the well section can obtain the skin factor model of the reservoir near the inclined well section of the well in the anisotropic reservoir, as shown in Eq. (26). Similarly, the skin factor model of vertical well section and horizontal well section in special cases can be obtained by the above method, as shown in Eqs. (27) and (28).

$$S_{\mathrm{di}}=\int_0^{L_{\mathrm{i}}}\frac{\beta h'}{L'_{\mathrm{i}}}\left(\frac{K'}{K'_{\mathrm{d}}}-1\right)\ln\left(\frac{\sqrt{\frac{K_u}{K_v}}\cdot\frac{r_{\mathrm{d}}(w)}{r_{\mathrm{w}}}+\sqrt{\frac{K_u}{K_v}\frac{r_{\mathrm{d}}^2(w)}{r_{\mathrm{w}}^2}+\frac{K_u}{K_v}-1}}{1+\sqrt{\frac{K_u}{K_v}}}\right)\mathrm{d}w \tag{26}$$

$$S_{\mathrm{dv}}=\int_0^{L_{\mathrm{v}}}\frac{\beta h'}{L'_{\mathrm{v}}}\left(\frac{K'}{K'_{\mathrm{d}}}-1\right)\ln\left(\frac{\sqrt{\frac{K_u}{K_v}}\cdot\frac{r_{\mathrm{d}}(w)}{r_{\mathrm{w}}}+\sqrt{\frac{K_u}{K_v}\frac{r_{\mathrm{d}}^2(w)}{r_{\mathrm{w}}^2}+\frac{K_u}{K_v}-1}}{1+\sqrt{\frac{K_u}{K_v}}}\right)\mathrm{d}w \tag{27}$$

$$S_{\mathrm{dh}}=\int_0^{L_{\mathrm{h}}}\frac{\beta h'}{L'_{\mathrm{h}}}\left(\frac{K'}{K'_{\mathrm{d}}}-1\right)\ln\left(\frac{\sqrt{\frac{K_u}{K_v}}\cdot\frac{r_{\mathrm{d}}(w)}{r_{\mathrm{w}}}+\sqrt{\frac{K_u}{K_v}\frac{r_{\mathrm{d}}^2(w)}{r_{\mathrm{w}}^2}+\frac{K_u}{K_v}-1}}{1+\sqrt{\frac{K_u}{K_v}}}\right)\mathrm{d}w \tag{28}$$

where K_u and K_v can be obtained from Eq. (10) when the well inclination angle and azimuth of the well section are known; L_{i}, L_{v} and L_{h} respectively represent the lengths of incline, vertical and horizontal well sections in the isotropic reservoir coordinate system; S_{dx}, S_{dv} and S_{dh} respectively represent the skin factor of reservoir damage near incline, vertical and horizontal well sections of complex-structure wells.

According to Eqs. (26)–(28), to calculate the total skin factor of complex-structure wells, it is also necessary to know the distribution of damage zone radius $r_{\mathrm{d}}(w)$ along the wellbore direction of each section and the permeability $K^{'}_{\mathrm{d}}$ after damage.

2.4. The maximum and distribution of damage zone radius

Damage zone radius can be expressed by skin factor:

$$r_{\mathrm{d}}=r_{\mathrm{w}}\cdot\mathrm{e}^{-S_{\mathrm{d}}} \tag{29}$$

According to the above equation, in special cases, when there is no pollution at the toe of the wellbore, the skin factor is 0 and the minimum damage zone radius r_{dmin} is the wellbore radius r_{w}. In fact, the value of damage zone radius is also difficult to obtain directly from the oil field, which generally needs to be obtained through indoor experiments (Li et al., 2022).

2.4.1. Calculation method of maximum damage zone radius

Jiang et al. (1995) established the empirical model of the maximum invasion depth of drilling fluid and completion fluid into the reservoir by processing the experimental data with multiple nonlinear regression:

$$r_{\mathrm{dmax}}=6.35\times10^{-4}\left(\frac{V_{\mathrm{f}}}{\varphi}\right)^{\frac{1}{3}}\Delta P^{\frac{1}{2}}\left[5.1+39.66K^{\frac{1}{2}}-34.35K^{\frac{1}{3}}\right] \tag{30}$$

where r_{dmax} is the maximum damage zone radius, m; V_{f} is the filtration loss of drilling fluid through 45.8 cm^2 filtering area under pressure difference ΔP within soaking time t, $\times 10^{-6}$ m^3; ΔP is difference between drilling fluid column pressure and formation pore pressure, $\times 10^6$ Pa; φ is the reservoir porosity, %; and K is the permeability of formation, $\times 10^{-12}$ m^2.

Wang et al. (2003) also obtained the empirical model for calculating the maximum invasion depth of working fluid of the horizontal well by multiple regression of experimental data:

$$r_{\mathrm{dmax}}=\frac{1}{4}\left(\Delta P-9.62\times10^4\mu-2.72002\times10^3K^{-1}+2.298\times K^{-2}+0.19\times K^{-3}+1.04\times10^5\right)^{\frac{1}{2}} \tag{31}$$

where μ is the viscosity of working fluid filtrate, $\times 10^{-3}$ Pa s; and K is the permeability of formation, $\times 10^{-15}$ m^2.

Qi et al. (1992) derived the model for calculating the invasion depth of drilling fluid into the reservoir:

$$r_{\mathrm{dmax}}=\sqrt{\frac{r_{\mathrm{w}}^2+\left(0.384r_{\mathrm{w}}\left(V_{\mathrm{fs}}t_{\mathrm{s}}+V_{\mathrm{fd}}t_{\mathrm{d}}\right)\times10^{-3}-S\cdot d_1^2\times10^{-6}\right)}{\pi d_1^2\varphi(1-S_{\mathrm{or}}-S_1-S_{\mathrm{monto}})}} \tag{32}$$

where V_{fs} and V_{fd} are static filtration and dynamic filtration within 30 min, $\times 10^{-6}$ m^3; $S=S(t_{\mathrm{s}})+S(t_{\mathrm{d}})+S_{\mathrm{out}}$, where t_{s} and t_{d} are the time of drilling fluid soaking and circulating in reservoir, d; $S(t_{\mathrm{s}})$, $S(t_{\mathrm{d}})$ and S_{out} respectively represent the amount of filtrate absorbed by the rock during soaking, the amount of filtrate absorbed by the rock during mud circulation and the amount of filtrate in the outer mud cake, $\times 10^{-6}$ m^3; d_1 is core diameter, $\times 10^{-3}$ m; S_{or}, S_1 and S_{monto} respectively represent residual oil saturation, residual saturation of rock pores after filtrate invasion and saturation of clay in original pore volume after water absorption and expansion, %.

All data required in the Eqs. (30)–(32) need to be obtained through experiments.

2.4.2. Distribution model of damage zone radius along the wellbore

Combined with the previous research experience, this paper proposes two models of damage zone radius distribution along the wellbore.

2.4.2.1. Empirical equation model. For the orthogonal planes of reservoirs with different directions along the wellbore, t in Eq. (32) can be written as the difference of well length L and w at this position divided by the average rate of penetration v, so as to obtain the distribution law of the damage zone radius along the wellbore direction:

$$\mathbf{r}_{\mathrm{d}} = \sqrt{\frac{r_{\mathrm{w}}^2 + \left(0.384 r_{\mathrm{w}}\left(V_{\mathrm{fs}} + V_{\mathrm{fd}}\right)\frac{l-\mathbf{w}}{v}\cdot 48 t_{\mathrm{d}} \times 10^{-3} - S\cdot d_1^2 \times 10^{-6}\right)}{\pi d_1^2 \varphi (1 - S_{\mathrm{or}} - S_1 - S_{\mathrm{monto}})}} \tag{33}$$

where $\mathbf{r}_{\mathrm{d}}$ is the vector of damage zone radius, m; l is the length of well section, m; and t_{d} is the time of well construction, d.

2.4.2.2. Oscillatory decreasing function model. Here, oscillation decreasing function is introduced to express the distribution of damage zone radius towards w direction, and the model is:

$$r_{\mathrm{d}}(w) = r_{\mathrm{dmax}}\cdot f(w)\cdot g(w) \tag{34}$$

where, r_{d} is the damage zone radius, m, and $r_{\mathrm{d}} \geq r_{\mathrm{w}}$; r_{dmax} is the maximum damage zone radius, m, and $r_{\mathrm{dmax}} = \mathbf{r}_{\mathrm{d}}(0)$; $f(w)$ is an oscillatory function and $g(w)$ is a decreasing function.

Take cosine type function as the oscillatory function $f(w)$:

$$f(w) = a\cdot[\cos(b \cdot \mathbf{w}) + c] \tag{35}$$

where a, b and c are both equation coefficients and they are all greater than 0. $a = 1/(1 + c)$; b is positively correlated with reservoir heterogeneity, whereas c is negatively correlated with reservoir heterogeneity, that is b~β and c~$-\beta$; and the values of b and c will respectively affect the fluctuation frequency and fluctuation range of damage zone radius along wellbore.

In isotropic reservoir, damage zone radius should be a pure linear decreasing distribution along wellbore root to toe without considering other factors. In anisotropic reservoirs, the decreasing function $g(w)$ is assumed to be in Table 1.

Where d is equation coefficient, which is also greater than 0 and correlated with the well section length.

It can be found that the Eq. (33) is one of parabolic decreasing functions. Combine the two functions and the oscillatory decreasing function model can be gotten. Then the distribution of damage zone can be obtained.

2.5. Equivalent permeability and damage zone radius conversion method

Consider that the fluid flow in different wellbore orthogonal plane ouv in equivalent isotropic reservoir follows plane radial flow:

$$Q_{\mathrm{ouv}} = \frac{2\pi K' L'_w \Delta P}{\mu_{\mathrm{o}} B_{\mathrm{o}} \ln\left(\frac{r'_{\mathrm{c}}}{r'_{\mathrm{w}}}\right)} \tag{36}$$

where Q_{ouv} is the rate of flow in an ouv plane, m^3/d; L'_w is equivalent thickness of reservoir in w direction in equivalent isotropic reservoir, m; ΔP is difference between drilling fluid column pressure and formation pore pressure, $\times 10^6$ Pa; μ_{o} is crude oil viscosity $\times 10^{-3}$ Pa s; B_{o} is volume factor of crude oil; and r'_{c} is equivalent oil drain radius in equivalent isotropic reservoir, m.

Table 1
Four kinds of the decreasing function.

Decreasing function	Function	Functional form
$g(w)$	$d\cdot(-\mathbf{w}+l)$	Liner
	$d\cdot\sqrt{(-\mathbf{w}+l)}$	Parabolic
	$e^{-d\cdot\mathbf{w}}$	Exponential
	$d\cdot\ln[(-\mathbf{w}+l+1)]$	Logarithmic

Suppose that the pressures of the well section at different positions from well root to toe are $P_1, P_2, P_3, \ldots, P_i, \ldots, P_n$, and the corresponding permeabilities are $K_1, K_2, K_3, \ldots, K_i, \ldots, K_n$. Then the total flow of the well is equal to the sum of the partial flows of each well section:

$$Q = \sum_{i}^{n} \frac{2\pi K'_i L'_{wi} \Delta P_i}{\mu_{\mathrm{o}} B_{\mathrm{o}} \ln\left(\frac{r'_{\mathrm{c}}}{r'_{\mathrm{w}}}\right)} \tag{37}$$

The equivalent origin permeability can be obtained from Eqs. (36) and (37):

$$K' = \frac{\sum_{i}^{n} K'_i L'_{wi} \Delta P_i}{L' \Delta P} \tag{38}$$

Generally speaking, reservoir damage will cause an additional pressure drop of the reservoir around the wellbore:

$$\Delta P_{\mathrm{s}} = S_{\mathrm{d}}\cdot\frac{141.2 Q \mu_{\mathrm{o}} B_{\mathrm{o}}}{K' L'} \tag{39}$$

where ΔP_{s} is additional pressure drop, $\times 10^6$ Pa.

Then the equivalent permeability after damage is:

$$K'_{\mathrm{d}} = \frac{\sum_{i}^{n} K'_i L'_{wi} (\Delta P_i - \Delta P_{si})}{L' \Delta P} \tag{40}$$

2.6. Skin factor model of complex-structure wells

By substituting Eqs. (34), (38) and (40) into Eqs. (26)–(28), the skin factor calculation models of inclined section, vertical section and horizontal section in complex-structure wells can be obtained respectively:

$$S_{\mathrm{di}} = \frac{\beta h'}{L'_{\mathrm{i}}} \frac{\Delta P_{\mathrm{s}}}{\Delta P - \Delta P_{\mathrm{s}}} \int_0^{L_{\mathrm{i}}} \ln\left(\frac{\sqrt{\frac{K_u}{K_v}}\cdot\frac{r_{\mathrm{d}}(w)}{r_{\mathrm{w}}} + \sqrt{\frac{K_u}{K_v}\frac{r_{\mathrm{d}}^2(w)}{r_{\mathrm{w}}^2} + \frac{K_u}{K_v} - 1}}{1 + \sqrt{\frac{K_u}{K_v}}}\right) \mathrm{d}w \tag{41}$$

$$S_{\mathrm{dv}} = \frac{\beta h'}{L'_{\mathrm{v}}} \frac{\Delta P_{\mathrm{s}}}{\Delta P - \Delta P_{\mathrm{s}}} \int_0^{L_{\mathrm{v}}} \ln\left(\frac{\sqrt{\frac{K_u}{K_v}}\cdot\frac{r_{\mathrm{d}}(w)}{r_{\mathrm{w}}} + \sqrt{\frac{K_u}{K_v}\frac{r_{\mathrm{d}}^2(w)}{r_{\mathrm{w}}^2} + \frac{K_u}{K_v} - 1}}{1 + \sqrt{\frac{K_u}{K_v}}}\right) \mathrm{d}w \tag{42}$$

$$S_{\mathrm{dh}} = \frac{\beta h'}{L'_{\mathrm{h}}} \frac{\Delta P_{\mathrm{s}}}{\Delta P - \Delta P_{\mathrm{s}}} \int_0^{L_{\mathrm{h}}} \ln\left(\frac{\sqrt{\frac{K_u}{K_v}}\cdot\frac{r_{\mathrm{d}}(w)}{r_{\mathrm{w}}} + \sqrt{\frac{K_u}{K_v}\frac{r_{\mathrm{d}}^2(w)}{r_{\mathrm{w}}^2} + \frac{K_u}{K_v} - 1}}{1 + \sqrt{\frac{K_u}{K_v}}}\right) \mathrm{d}w \tag{43}$$

For dual horizontal wells, multilateral wells and such complex-structure wells including one more well section, the overall reservoir damage cannot be evaluated by a simple numerical superposition of skin factors of all the branch well sections, but should be equivalent conversion on damage zone radius then recalculate the skin factor as a whole.

The converted damage zone radius of the whole well can be converted by:

$$r_d = \frac{\sum_i^n \int r_d(w)_i \mathrm{d}w}{L} \tag{44}$$

where n is the number of well section of complex-structure well; L is the total length of well, m.

Therefore, the skin factor of the whole complex-structure well is:

$$\begin{cases} S_d = \dfrac{\beta h'}{L'} \dfrac{\Delta P_s}{\Delta P - \Delta P_s} \displaystyle\int_0^L \ln\left(\dfrac{\sum_i^n \frac{r_{di}}{r_w}}{L}\right) \mathrm{d}w \\ r_{di}(w_i) = r_{di\ max} \cdot f(w_i) \cdot g(w_i) \\ \displaystyle\sum_i^n \frac{r_{di}}{r_w} = \sum_i^n \int_0^{L_i} \left(\dfrac{\sqrt{\frac{K_{ui}}{K_{vi}}} \cdot \frac{r_{di}(w_i)}{r_w} + \sqrt{\frac{K_{ui}}{K_{vi}} \frac{r_{di}^2(w_i)}{r_w^2} + \frac{K_{ui}}{K_{vi}} - 1}}{1 + \sqrt{\frac{K_{ui}}{K_{vi}}}} \right) \mathrm{d}w_i \end{cases} \tag{45}$$

By substituting the above skin factor model into the general production model, the modified production model of the corresponding well section or the whole complex-structure well considering reservoir damage can be finally calculated.

2.7. A new modified production model of horizontal well considering reservoir formation damage

Modifying the Joshi's horizontal well production model (Joshi, 1988) by the established skin factor model, and a new horizontal well production model considering reservoir damage is obtained:

$$Q = \frac{2\pi K_h' h' \Delta P}{\mu_o B_o \left[\ln\left(\frac{a' + \sqrt{a'^2 - (L'/2)^2}}{L'/2} \right) + \frac{\beta h'}{L'} \left[\ln\left(\frac{\beta h'}{2\pi r_w'} \right) + S_d \right] \right]} \tag{46}$$

where $a' = L'/2\sqrt{1/2 + \sqrt{1/4 + (2r_e'/L')^4}}$.

3. Field case and model application

3.1. Field case 1: Horizontal well P314

Horizontal well P314 is located in the west of 7th zone of Shengli Gudong Oilfield (China). The structure diagrammatic sketch and basic data of P314 well are shown in Fig. 7 and Table 2.

By substituting the known data into Eq. (43), the skin factor S_d of this horizontal well can be calculated. Then substituting S_d into Eq. (46), the well production Q_h can be obtained.

3.2. Field case 2: Herringbone well CF1

Herringbone well CF1 is located in Bohai Oilfield (China). The structure diagrammatic sketch and basic data of CF1 well are shown in Fig. 8 and Table 3.

By substituting the known data of main and branch wells into Eq. (43) respectively, the skin factor S_{di} of each branch well can be calculated. Then substitute S_{di} into Eq. (46) to obtain the well production Q_{hi} of each branch well. The total well production can be gotten by adding the Q_{hi} of all branch wells. And the equivalent damage zone radius and total skin factor of this whole herringbone well can be obtained by Eqs. (44) and (45).

4. Results

4.1. Reservoir formation damage simulation

4.1.1. Horizontal well P314

The reservoir damage zone radius and local skin factor distribution along the wellbore of well P314 were calculated through the model, and the results are shown in Figs. 9 and 10.

From the results, it can be seen that the maximum damage zone

Table 2
Basic data of horizontal well P314.

Data	Value and Unit
L_h	315 m
h	171.8 m
r_w	0.18 m
r_{eh}	535.2 m
μ_o	65 × 10^{-3} Pa s
B_o	1.07
K_h	575.1 × 10^{-15} m^2
φ	0.34
β	3.5
P_e	13.3 × 10^6 Pa
P_{wf}	11 × 10^6 Pa
ΔP_s	2 × 10^6 Pa
φ	160°
θ	90°

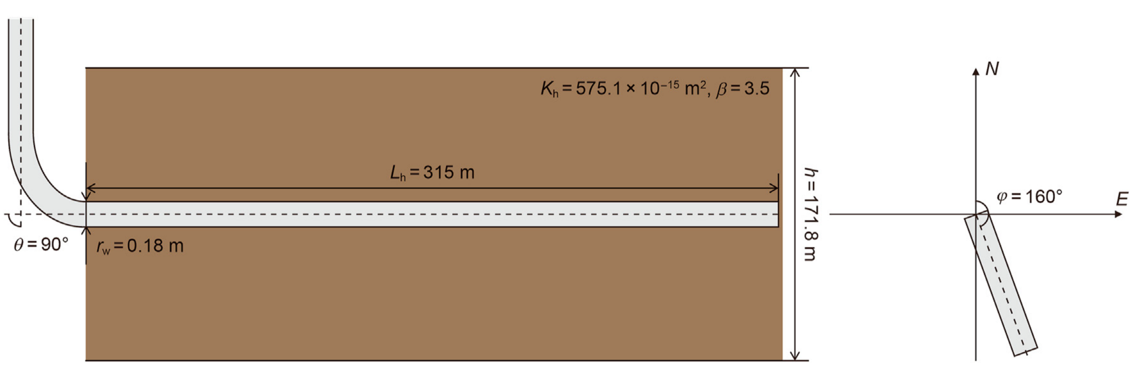

Fig. 7. Structure diagrammatic sketch of horizontal well P314.

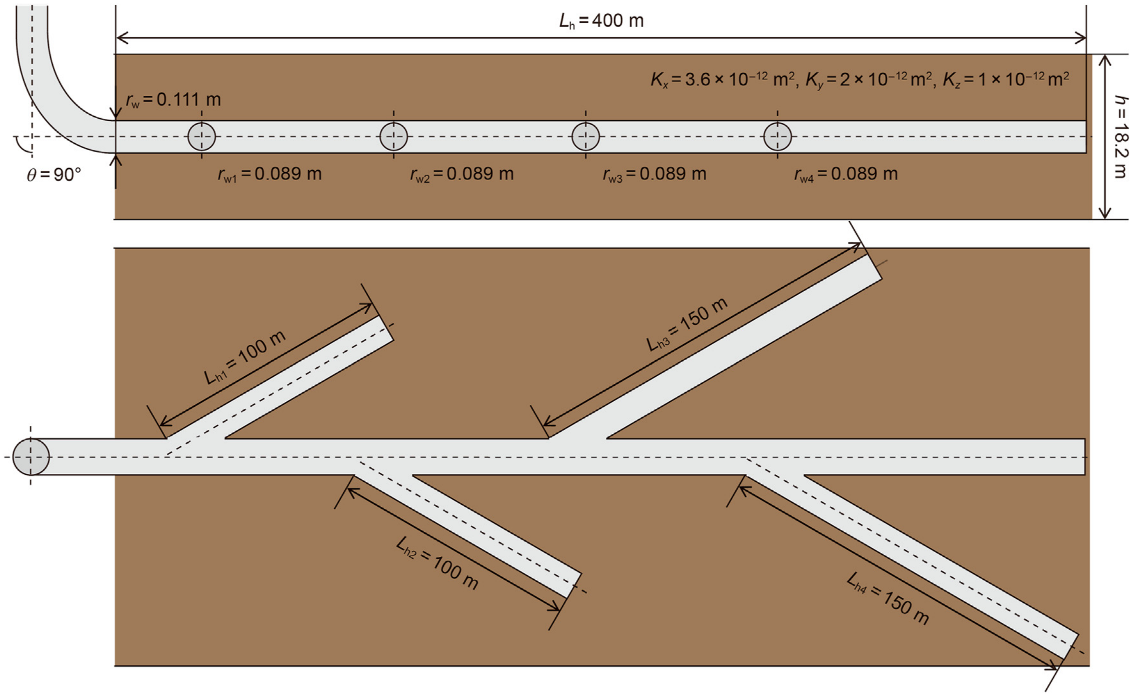

Fig. 8. Structure diagrammatic sketch of herringbone well CF1.

Table 3
Basic data of herringbone well CF1.

Symbol	Value and Unit
L_h	400 m
L_{h1}	100 m
L_{h2}	100 m
L_{h3}	150 m
L_{h4}	150 m
r_w	0.111 m
r_{w1}, r_{w2}, r_{w3}, r_{w4}	0.089 m
r_e	319 m
h	18.2 m
K_x	3.6×10^{-12} m^2
K_y	2×10^{-12} m^2
K_z	1×10^{-12} m^2
K_d	0.31×10^{-12} m^2
μ_o	380×10^{-3} Pa s
P_e	14.4×10^6 Pa
ΔP	1×10^6 Pa

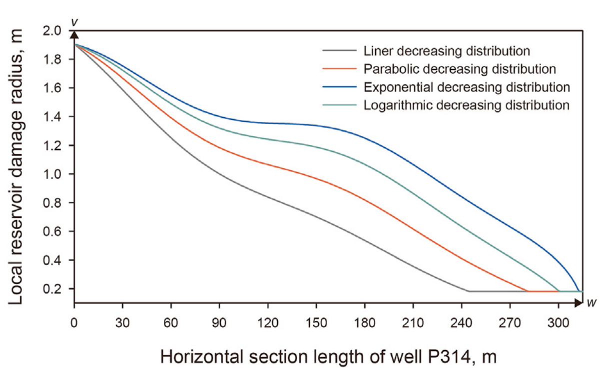

Fig. 9. Reservoir damage zone radius distribution along wellbore of well P314.

radius of well P314 is 1.9 m and the minimum is approximate to r_w.

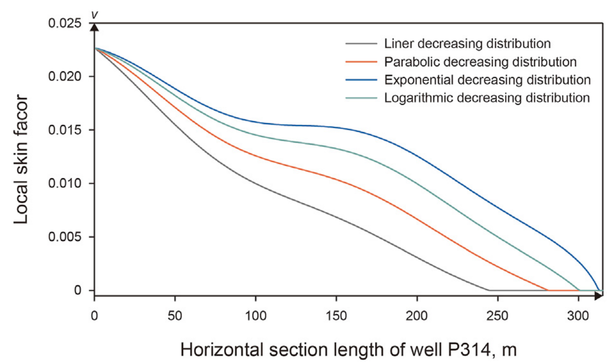

Fig. 10. Local skin factor distribution along wellbore of well P314.

The local skin factor decreases from the root ($x = 0$ m) to the toe ($x = 315$ m), mainly because the formation near the well root has the longest contact time with the drilling and completion fluid, so the damage and local skin factor is the largest. Whereas, the contact time between the formation near the well toe and external fluid is short, so that the damage and local skin factor is minimal.

Then the total skin factor results were calculated by Eq. (43), as shown in Table 4.

The reservoir formation damage simulation of well P314 is shown in Fig. 11.

Fig. 11 well clearly shows the uneven decreasing distribution of reservoir damage from the root to toe of the wellbore and the elliptical distribution of damage zone in the orthogonal plane of the wellbore in anisotropic reservoir of the well P314, which certifies that this model can well simulated the reservoir formation damage of the complex-structure well.

4.1.2. Herringbone well CF1

Here, the parabolic oscillatory decreasing function model was chosen to represent the damage zone distribution. The damage

Table 4
Total skin factor calculated results of well P314.

Decreasing function	S_d
Liner	2.3066
Parabolic	2.9816
Exponential	4.1698
Logarithmic	3.6217

zone radius and local skin factor distribution of the main well and four branch wells are shown in Figs. 12 and 13.

The maximum damage zone radius of the main well and each branch well are respectively 0.5800 m, 0.5065 m, 0.4227 m, 0.3470 m and 0.2553 m. The single skin factor of each well section, the total skin factor and the equivalent damage zone radius of the whole well are shown in Table 5.

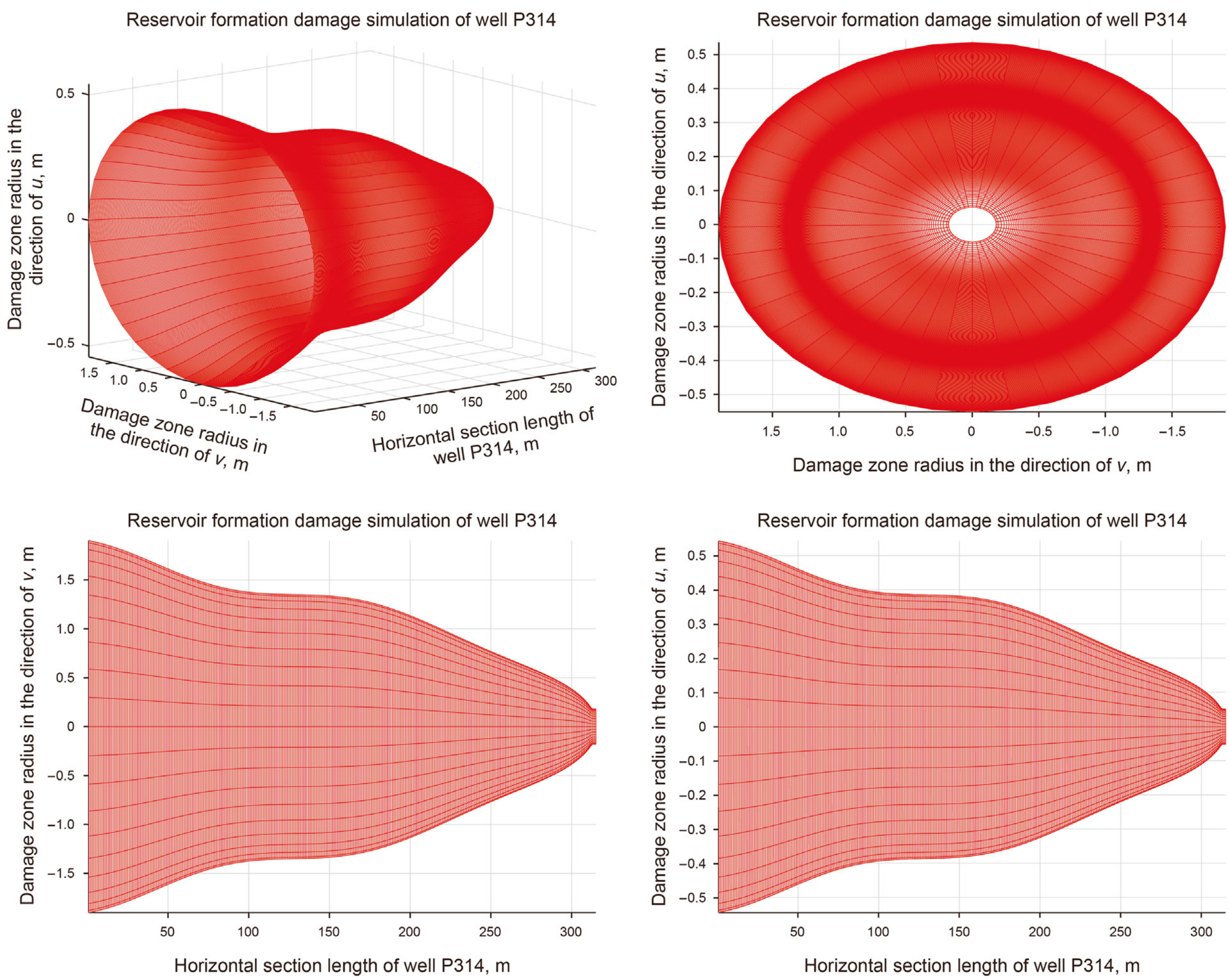

Fig. 11. Reservoir formation damage of well P314 simulated by the model.
Note: This figure is simulated by the model with the exponential decreasing function.

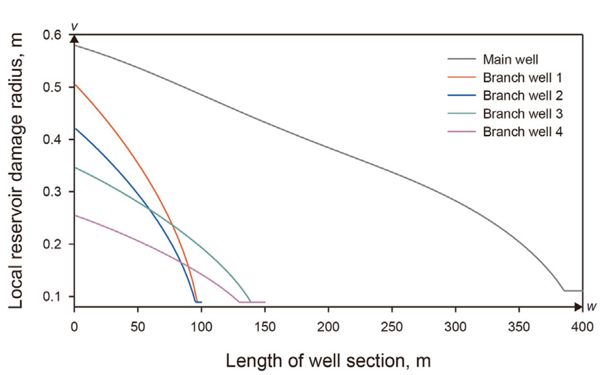

Fig. 12. Damage zone radius distribution along wellbore of well CF1.

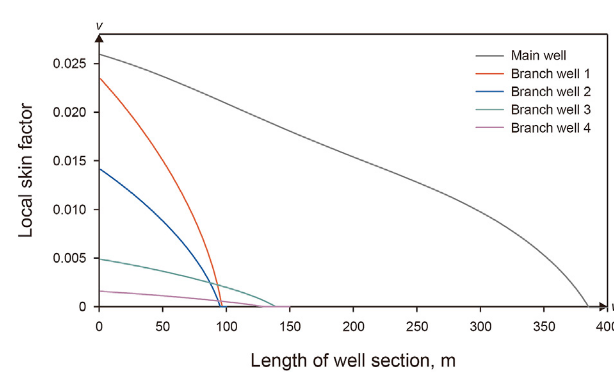

Fig. 13. Local skin factor distribution along wellbore of well CF1.

Table 5
Skin factor simulation results of well CF1.

Symbol	Value
S_{dm}	1.4099
S_{db1}	1.0421
S_{db2}	0.8103
S_{db3}	0.3984
S_{db4}	0.1169
S_d	1.8974
r_{de}	0.3013

4.2. Production prediction and model accuracy analysis

Production of horizontal well P314 was predicted by the new horizontal well production model and Joshi's model respectively and the results are shown in Table 6.

It can be seen from Tables 4 and 6 that the four decreasing functions have similar effects on skin factor and production simulation results. Among them, the production simulated by the damage zone distribution model with parabolic, exponential and logarithmic oscillatory decreasing function are all closer to the field production of well P314 than liner oscillatory decreasing function model. Comparing to Joshi's horizontal well production model, the modified models have higher accuracy mainly because the Joshi's model didn't consider the negative effect to the well production caused by reservoir formation damage, so that the corresponding predicted production is higher than the reality.

Equally considering the reservoir damage in the production prediction, that is taking into account the skin factor in the prediction, the production results of each well section of well CF1 are shown in Table 7, in which the production data predicted by the model, which did not consider the reservoir damage, is from the reference (Fan et al., 2006; An et al., 2008).

From the results simulated in Table 7, it can be seen that the production prediction result simulated by the model, after considering the reservoir formation damage, is also closer to the field measured production than the prediction result, which doesn't consider the reservoir formation damage.

From the above two field cases, the model for evaluating reservoir formation damage of complex-structure wells has the convincing accuracy, and the relative error is as low as 10% comparing with the filed data.

5. Discussion

5.1. Uneven distribution of reservoir damage along the wellbore

It is generally accepted that the damage zone radius and local skin factor at the toe of the wellbore is the smallest since the contact time between reservoir and drilling fluid is the shortest. Correspondingly, damage zone radius and local skin factor at the root of wellbore are both the largest because the contact time between reservoir and working fluid is the longest, so the damage is the most serious. Moreover, the distribution of damage zone radius along the wellbore direction is not simple linear distribution because of reservoir anisotropy no matter for any type wells (Furui et al., 2003, 2004). It is also indicated from the reservoir formation damage simulation results of the first field case P314 well that the damage zone distribution model with liner oscillatory decreasing function has lower accuracy comparing to the other three functions.

The heterogeneity of permeability along the wellbore is the main factor leading to the heterogeneity of reservoir damage, as well as skin factor. In addition, many factors such as properties of drilling and completion fluid and construction parameters will also aggravate the heterogeneity. Therefore, reservoir damage shows a decreasing and also uneven distribution from root to toe of wellbore, as shown in Fig. 14. Not considering the serious loss of working fluid caused by special fractures around the well, the oscillatory decreasing function model can approximate the quantitative expression of damage zone radius distribution.

5.2. Skin factor of single well section or the whole well in complex-structure wells

Skin factor is an important technical index to evaluate the reservoir formation damage of wells, which provides a reference for the design of stimulation measures in the oilfield. In the field, the total skin factor, which is under the combined action of various factors, is usually obtained by pressure recovery test and pressure drop test. For evaluating the reservoir damage, there is only one total skin factor for one well, especially for the complex-structure wells which include multiple well sections. Single skin factor or production for one well section can be calculated individually, and the total well production is equal to the sum of the productions of each well section, whereas total skin factor cannot be same as the sum of single skin factors of each well section. Just like the skin factor simulation results of the second field case CF1 well in Table 5. The skin factor of main well and branch wells of CF1 well can be all respectively calculated. Of course, the main well has the most serious reservoir damage, and the reservoir damage of the other four branch wells decreases successively along the main well bore. The total skin factor of the whole well was calculated by Eq. (45), so it is not an easy composition of skin factors of each well section.

5.3. Influence of model input factors on reservoir damage degree

5.3.1. Reservoir anisotropy

Fig. 15 shows the relationship between local skin factor and well section length with different formation anisotropy coefficients.

It can be seen that the local skin factor at the same position of this well section increases with the increase of β, and then the total skin factor of the whole well section also increases. This is because the flowing resistance in the vertical direction increases due to the decrease of the vertical permeability of the reservoir, which would eventually reduce the production of the well.

Table 6
Production predicted results of well P314.

Calculation method		Production, m^3/d	Relative error, %
Measured production		2.1875	0.00
Joshi's model		3.3009	50.90
Modified model with the decreasing function of	Liner	2.5066	14.59
	Parabolic	2.3418	7.05
	Exponential	2.0988	4.05
	Logarithmic	2.2043	0.77

Table 7
Production predicted results of well CF1.

Type	Production		
	Predicted by model, m^3/d		Measured in field, m^3/d
	Not considering reservoir damage	Considering reservoir damage	
Main well	24.90	23.21	/
Branch well 1	9.20	8.49	/
Branch well 2	8.43	7.92	/
Branch well 3	12.99	12.65	/
Branch well 4	13.98	13.87	/
The whole well	69.50	66.14	64.00
Relative error, %	8.59	3.34	0

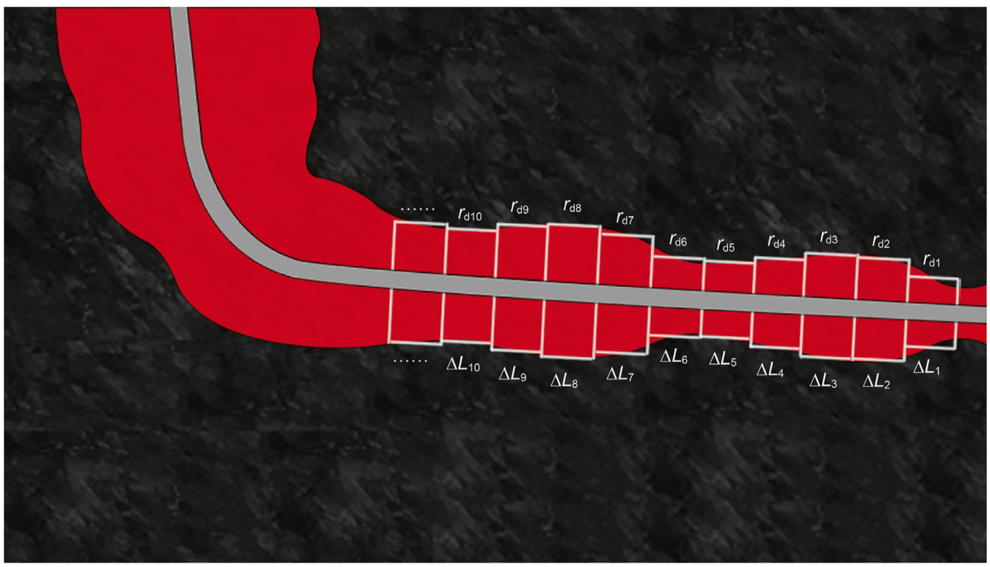

Fig. 14. Schematic diagram of reservoir damage zone radius distribution along wellbore in complex-structure wells.

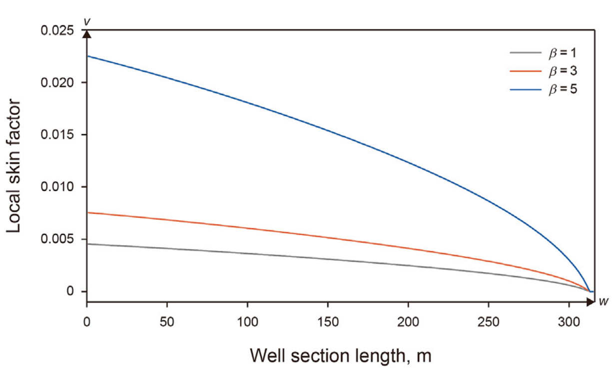

Fig. 15. Relationship curve between local skin factor and well section length with different formation anisotropy coefficients.

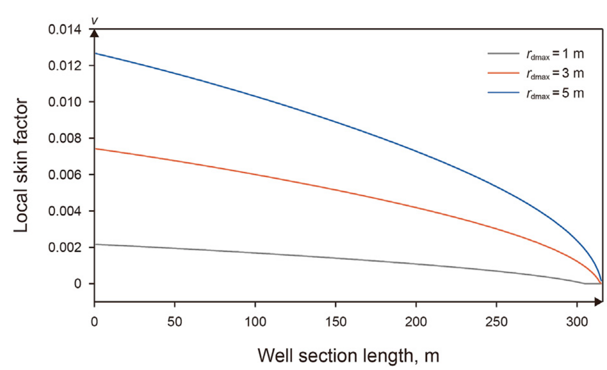

Fig. 16. Relationship curve between local skin factor and well section length with different maximum damage zone radius.

5.3.2. Maximum damage zone radius

Fig. 16 shows the relationship between local skin factor and well section length with different maximum damage zone radius (maximum invasion depth of working fluid).

It can be seen that the local skin factor at the same position of the well section increases with the increase of the maximum damage zone radius, and then the total skin factor of the whole well section also increases. The reason is that with the increase of maximum invasion depth of external working fluid, the flowing resistance near the well section also increases, finally resulting in the reduction of well production. Therefore, it should be paid attention to the reservoir protection in the process of well drilling and completion.

5.3.3. Permeability

Fig. 17 shows the relationship between local skin factor and well section length with different permeability.

It can be seen that the local skin factor at the same position of the well section increases with the increase of the permeability, and

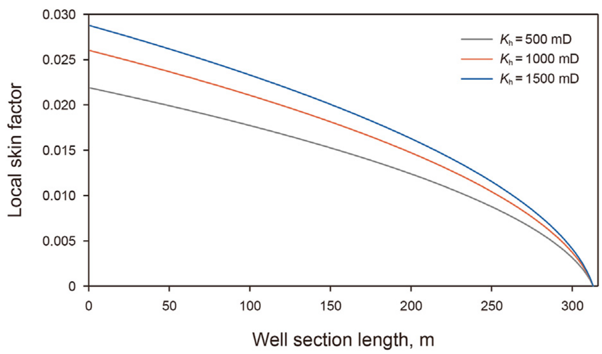

Fig. 17. Relationship curve between local skin factor and well section length with different permeability.

then the total skin factor of the whole well section also increases. It is that with the increase of permeability, the fluid flow and also the working fluid invasion both become easier. Conversely, the formation damage caused by working fluid invasion in the tight reservoir is usually very slight.

5.4. Limitations of model application and future work

The skin factor model established by subsection and superposition method in this paper can quantitatively evaluate reservoir formation damage of complex-structure wells. Considering the reservoir damage, the improved production model can more accurately predict the production, optimize the drilling fluid suitable for the reservoir, and also provide guidance for plug removal and stimulation. However, it also has some limitations due to the assumptions and modeling methods. First, the model is not very suitable for evaluating the well section near the reservoir with large and special fractures, as the important parameter r_d is obtained from Eqs. (30)–(34), among them, whose calculation is based on the classic laboratory core damage experiment. If there are large or special fractures in the formation, it will cause massive loss of working fluid, which cannot be very precisely tested by the experiment. So, there will be great difference between the data of working fluid loss testing in laboratory and field, and then the special situation cannot be well reflected by those empirical equations. Equally, the reservoir damage of tight and shale reservoirs cannot be greatly evaluated by the model, because it is difficult for drilling fluid to invade in these tight formations. What's more, the drilling fluid loss in core damage experiment is also difficult to test in laboratory, which further influences to analyze the invasion depth and the maximum damage zone radius. Moreover, there is also one further point to make, that is the modified production prediction model is not suitable for evaluating the reservoir damage of gas wells. Because the production model adopts the condition of constant flow, while the gas wells give tacit consent to the condition of constant pressure.

For the long-term reservoir protection is a wish that petroleum engineers have been trying to achieve and is subjected to further promotion. Reservoir damage is inevitable, so subsequent damage removal, like acidizing, is particularly important. It is very important to know the shape and range of damage zone for the design and effect of plug removal. In the future, engineers can make improvements in accuracy and visualization of model calculation results. Additionally, in anisotropic reservoirs, the permeability in the direction of main stress and the anisotropic coefficient are essential data for model calculation, so, considering how to simply and quickly to obtain the necessary parameters is of the essence.

6. Conclusions

Due to the reservoir anisotropy, the reservoir formation damage for complex-structure wells would be more serious and complex. Therefore, quantitatively evaluating the reservoir damage is particularly important for the subsequent selection of stimulation measures and reservoir protection for complex-structure wells.

In this paper, the anisotropic reservoir is transformed into the equivalent isotropic reservoir by coordinate transformation method, which is more convenient for the study of heterogeneous reservoir. And the local skin factor in the orthogonal plane of wellbore is derived. Then oscillation decreasing function models and empirical equation models are separately proposed considering the uneven distribution of reservoir damage along the wellbore, which further improves the pure linear distribution of damage zone along the wellbore as we all know. Finally, total skin factor can be obtained by integrating the local skin factors in the whole well, which is suitable for evaluating reservoir damage in complex-structure wells with arbitrary trajectory. For the complex-structure wells with multiple well sections, the conversion method of the damage zone radius should be converted to get the total skin factor rather than simply adding the skin factor of each well section. Combining the total skin factor model with the production prediction model, the production of complex-structure wells can be predicted more accurately.

The field application cases clearly show that the accuracy of the skin factor model is as high as 90%, and the results also show that the distribution damage zone radius model with linear decreasing function has higher error compared with the parabolic, exponential and logarithmic decreasing function.

Declaration of competing interest

The authors declare that they have no known competing financial interests or personal relationships that could have appeared to influence the work reported in this paper.

Acknowledgements

This work is financially supported by National Natural Science Foundation of China (Grant No. 52004297 and Grant No. 51991361) and China Postdoctoral Science Foundation (Grant No. BX20200384). We would like to acknowledge the editor and reviewers from *Petroleum Science* for their time and effort on improving the quality of this paper.

References

Aadnoy, B.S., Cooper, L., Miska, S.Z., et al., 2009. Advanced Drilling and Well Technology. Society of Petroleum Engineers.

Ahmadi, H., Clarkson, C.R., Hamdi, H., et al., 2020. Analysis of communicating multi-fractured horizontal well production data using the dynamic drainage area concept. In: SPE Canada Unconventional Resources Conference, September 2020. Virtual. https://doi.org/10.2118/199987-ms.

Alghazal, M., Alshakhs, M., Bouaouaja, M., 2020. Technology integration to assess end-point oil saturation of the relative permeability curves. In: International Petroleum Technology Conference, January 2020. Dhahran, Kingdom of Saudi Arabia. https://doi.org/10.2523/iptc-19614-ms.

An, Y., Wu, X., Han, G., Li, F., 2008. A productivity prediction model for the complex well with formation damage. Petrol. Explor. Dev. 35 (5), 625–629 (in Chinese).

Basquet, R., Alabert, F.G., Caltagirone, J.P., et al., 1998. A Semi-analytical Approach for Productivity Evaluation of Wells with Complex Geometry in Multilayered Reservoirs. In: SPE Technical Conference & Exhibition, September 1998. New Orleans, Louisiana. https://doi.org/10.2118/49232-MS.

Besson, J., 1990. Performance of slanted and horizontal wells on an anisotropic medium. In: European Petroleum Conference, October 1990. The Hague, Netherlands. https://doi.org/10.2118/20965-ms.

Dulkarnaev, M.R., Malyavko, E.A., Semyonova, E.E., et al., 2021. The use of quantum dot inflow tracers in multi-well reservoir production surveillance and inter-well diagnostics. In: SPE Symposium: Petrophysics XXI. Core, Well Logging,

and Well Testing, June 2021. Virtual. https://doi.org/10.2118/208430-ms.
Fan, Y., Han, G., Yang, C., 2006. Production forecast for herringbone well and optimum configuration of lateral holes. Acta Pet. Sin. 27 (4), 101–104 (in Chinese).
Frick, T.P., Economides, M.J., 1993. Horizontal well damage characterization and removal. SPE Prod. Facil. 8 (1993), 15–22. https://doi.org/10.2118/21795-PA.
Furui, K., Zhu, D., Hill, A.D., 2003. A rigorous formation damage skin factor and reservoir inflow model for a horizontal well. SPE Prod. Facil. 18 (2003), 151–157. https://doi.org/10.2118/84964-pa.
Furui, K., Zhu, D., Hill, A.D., 2004. A new skin factor model for gravel-packed completions. In: SPE Annual Technical Conference and Exhibition, September 2004. Houston, Texas. https://doi.org/10.2118/90433-ms.
Hasan, A.R., Kabir, C.S., Wang, X., 2009. A robust steady-state model for flowing-fluid temperature in complex wells. SPE Prod. Oper. 24 (2009), 269–276. https://doi.org/10.2118/109765-PA.
Hassan, A., Mahmoud, M., Al-Majed, A., et al., 2020. A New Technique to Quantify the Productivity of Complex Wells Using Artificial Intelligence Tools. In: International Petroleum Technology Conference, January 2020. Dhahran, Kingdom of Saudi Arabia. https://doi.org/10.2523/IPTC-19706-Abstract.
Hawkins, M., 1956. A note on the skin effect. J. Petrol. Technol. 8 (1956), 65–66. https://doi.org/10.2118/732-G.
He, Y., Liu, Y., Cai, H., et al., 2022. Fine characterisation of remaining oil using time-varying numerical simulation: experimental study. In: Characterisation in Model, and Application in QHD Oilfield. Offshore Technology Conference Asia, March 2022. Virtual and Kuala Lumpur, Malaysia. https://doi.org/10.4043/31410-ms.
Hu, D., Li, Y., Hu, S., et al., 2022. Data-driven injection/production optimization for horizontal well pattern in a complex carbonate oilfield. In: Offshore Technology Conference Asia, March 2022, Virtual and Kuala Lumpur. Malaysia. https://doi.org/10.4043/31428-ms.
Jenny, P., Lunati, I., 2009. Modeling complex wells with the multi-scale finite-volume method. J. Comput. Phys. 228 (3), 687–702. https://doi.org/10.1016/j.jcp.2008.09.026.
Jiang, G., Yan, J., Wu, X., 1995. Mathematical model for the calculation of invasion depth of solid particles of completion fluid into reservoir. Drill. Fluid Complet. Fluid 12 (2), 66–73 (in Chinese).
Jiang, G., Sun, J., He, Y., et al., 2021. Novel water-based drilling and completion fluid technology to improve wellbore quality during drilling and protect unconventional reservoirs. Engineering 18, 129–142. https://doi.org/10.1016/j.eng.2021.11.014.
Joshi, S.D., 1986. Augmentation of well productivity using slant and horizontal wells. In: SPE Annual Technical Conference and Exhibition, October 1986. New Orleans, Louisiana. https://doi.org/10.2118/15375-ms.
Joshi, S.D., 1987. A review of horizontal well and drainhole technology. In: SPE Annual Technical Conference and Exhibition, September 1987. Dallas, Texas. https://doi.org/10.2118/16868-ms.
Joshi, S.D., 1988. Augmentation of well productivity with slant and horizontal wells (includes associated papers 24547 and 25308). J. Petrol. Technol. 40 (6), 729–739. https://doi.org/10.2118/15375-pa.
Joshi, S.D., 1994. Horizontal wells: successes and failures. J. Can. Pet. Technol.. No Pagination Specified 33 (1994). https://doi.org/10.2118/94-03-01.
Joshi, S.D., 2003. Cost/benefits of horizontal wells. In: SPE Western Regional/AAPG Pacific Section Joint Meeting, May 2003. Long Beach, California. https://doi.org/10.2118/83621-ms.
Kang, H., Song, X., Dai, K., et al., 2021. Flow study of fractured well based on conformal mapping. China Mining Magzine 30 (3), 167–171 (in Chinese).
Kantaatmadja, B.P., Jiang, L., Ralphie, B., et al., 2019. Hydrocarbon identification and evaluation in a bioturbated reservoir with new-generation pulsed neutron technology. In: SPE/IATMI Asia Pacific Oil & Gas Conference and Exhibition, October 2019. Bali, Indonesia. https://doi.org/10.2118/196364-ms.
Klemetsdal, Ø., Berge, R., Lie, K.A., et al., 2017. Unstructured gridding and consistent discretizations for reservoirs with faults and complex wells. In: SPE Reservoir Simulation Conference, February 2017. Montgomery, Texas, USA. https://doi.org/10.2118/182666-MS.
Li, Y., Jiang, G., Li, X., et al., 2022. Quantitative investigation of water sensitivity and water locking damages on a low-permeability reservoir using the core flooding experiment and NMR test. ACS Omega 7 (5), 4444–4456. https://doi.org/10.1021/acsomega.1c06293.
Liu, Y., Guo, F., Tu, B., et al., 2005. Measuring method for anisotropic permeability by non-uniform radial flow in a whole core. Acta Pet. Sin. 26 (6), 66–68 (in Chinese).
Mehrabi, M., Miska, S., Merlo, A., 2014. Complex Wells: New Perspective on the Selection of Optimal Drillpipe. In: IADC/SPE Drilling Conference and Exhibition, March 2014. Fort Worth, Texas, USA. https://doi.org/10.2118/167947-MS.
Moreno, J.C., Gurpinar, O.M., Bradley, D.C., et al., 2006. Optimized workflow for designing complex wells. In: SPE Europec/EAGE Annual Conference and Exhibition, June 2006. Vienna, Austria. https://doi.org/10.2118/99999-MS.
Peaceman, D.W., 1983. Interpretation of well-block pressures in numerical reservoir simulation with nonsquare grid blocks and anisotropic permeability. Soc. Petrol. Eng. J. 23, 531–543. https://doi.org/10.2118/10528-pa.
Poe Jr., B.D., Vacca, H., Benjamin, A., et al., 2012. Production decline analysis of horizontal wells intersecting multiple transverse vertical hydraulic fractures in low-permeability shale reservoirs. In: SPE Annual Technical Conference and Exhibition, October 2012. San Antonio, Texas, USA. https://doi.org/10.2118/160149-ms.
Qi, H., Pu, C., Luo, Z., 1992. Calculation method of drilling fluid invasion depth into reservoir. Drill. Fluid Complet. Fluid 9 (6), 20–22 (in Chinese).
Sau, R., Goodrow, A., Rockwell, M., et al., 2014. An integrated software technology based on research and field application for completion, stimulation and fluid placement design in complex wells. In: International Petroleum Technology Conference, December 2014. Kuala Lumpur, Malaysia. https://doi.org/10.2523/IPTC-17870-MS.
Smith, R.K., Sawyer, W.K., Esposito, P.R., 1981. The effect of anisotropy and vertical fracture penetration on production decline curves for low permeability gas wells. In: SPE Eastern Regional Meeting, November 1981. Columbus. Ohio. https://doi.org/10.2118/10369-ms.
Sun, E., 2020. Horizontal well productivity of anisotropic reservoir considering reservoir pollution. J. Shengli Coll. Ch. Univ. Petrol. 34 (4), 19–22. doi:10.3969/j.issn.1673-5935.2020.04.005 (in Chinese).
Thomas, L.K., Todd, B.J., Evans, C.E., et al., 1998. Horizontal well IPR calculations. PE Res Eval & Eng 1 (5), 392–399. https://doi.org/10.2118/51396-PA.
Wang, S., Hu, S., Liu, G., 2003. Mathematical model of horizontal well drilling and completion fluid damage to oil and gas reservoirs. Special Oil Gas Reservoirs 10 (4), 65–68 (in Chinese).
Wang, Z., Li, Z., Zhao, Z., 2009. Analysis of influence factors on productivity of horizontal well. Fault-Block Oil Gas Field 16 (3), 58–61 (in Chinese).
Wu, M., Zhu, J., Li, L., et al., 2020. Calculation of perforated vertical and horizontal well productivity in low-permeability reservoirs. SPE Drill. Complet. 35 (2), 218–236. https://doi.org/10.2118/198904-pa.
Wu, X., An, Y., Li, F., 2008. Productivity of horizontal gas well considering the influence of reservoir damage. Nat. Gas. Ind. 28 (7), 78–80 (in Chinese).
Zhang, Z., Yan, J., 2001. Study on the calculation method of the influence of reservoir damage on the productivity of highly deviated directional wells. Oil Drilling & Prod. Technol. 23 (6), 40–43. https://doi.org/10.13639/j.odpt.2001.06.012 (in Chinese).